IMPACT OF TURBULENCE ON THE CONTROL OF A HYDROKINETIC TURBINE

Robert J. Cavagnaro
University College Cork / HMRC. Cork, Ireland
University of Washington / NNMREC, Seattle, WA
rcav@uw.edu

ABSTRACT

A method for linearizing the first-order dynamics of a fixed-pitch, vertical axis hydrokinetic turbine about an operating point is detailed. The system's frequency response to turbulence and controller action is determined. Turbine parameters contributing to its dynamics are described and the effects on system response of geometrically scaling a turbine are explored. The turbine's sensitivity to turbulence across a wide frequency band is compared to the turbulent kinetic energy (TKE) present in a tidal channel across the same frequency band. The turbine is found to be most sensitive to low-frequency turbulence and control action perturbations, with decreasing gain at higher frequencies. Larger sized turbines are shown to have a lower magnitude response over a narrower frequency band. The turbine is shown to be more responsive to the most energetic turbulence frequencies. This method of analysis and subsequent results can inform controller design aspects such as the determination of control action frequency and magnitude.

INTRODUCTION

Control systems are essential to optimize power generation from hydrokinetic turbines. Turbine control options are dictated by the system layout: turbine dimensions, generator type, grid connection, orientation relative to flow, and ability to pitch blades are the major parameters that determine how the performance of the turbine can be regulated. Additionally, considerations such as operation in isolation or as part of an array will influence the control strategy. Currently, several lines of research are active in leveraging the similarities to wind turbines to develop analogous control techniques (Cavagnaro, et al., 2014; Whitby & Ugalde-Loo, 2014). As differences between the marine and atmospheric environments are numerous, there is no guarantee a controller suitable for operation in air will be viable for a turbine operating in water. Key differences influencing turbine control between working fluids of wind and water are the higher density and viscosity, slower speed, and different magnitudes and frequencies of turbulence in water. These differences manifest in hydrokinetic turbines that are, compared to their wind analogues extracting the same power, smaller in area, are subjected to higher degrees of damping forces, and are influenced by the added mass of water on the surface of blades. The goal of this study is to focus on a subset of these aspects: to determine the impacts of turbulence present in a high-energy marine environment on the dynamic response and control of a hydrokinetic turbine, and determine which turbine parameters can be adjusted in the design phase to yield a desired response. This analysis is intended to be a first step in the design of a suitable controller. A turbine layout with limited complexity is chosen and simplifying assumptions regarding its dynamics are utilized to create a first-order estimate of its response.

METHODOLOGY

1. THE DOE RM2 HYDROKINETIC TURBINE MODEL

The US Department of Energy Reference Model 2 (RM2) hydrokinetic turbine was chosen to analyse dynamic response to turbulence. The turbine design (Fig. 1) consists of a fixed-pitch vertical axis three-bladed turbine rated at 50 kW in 2 m/s flow (Barone et al., 2011). The turbine's characteristic curve, inertia, and damping coefficient have been previously estimated and parameters are provided in Table 1 (Neely et al., 2013).

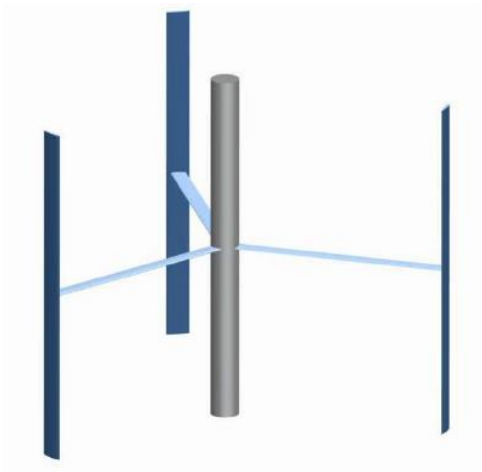

FIGURE 1: DOE RM2 rotor schematic from Barone et al. (2011).

Parameter	Value	Units
R_t	3.23	m
A_t	31.22	m^2
J	8407	kg-m^2
B	37.26	Nm-s/rad

TABLE 1: DOE RM2 Turbine Parameters

A first-order differential equation describes the relationship between the turbine's rotation rate (ω_t), effective total rotational moment of inertia (J), hydrodynamic torque (τ_h), control torque (τ_c), and effective damping coefficient (B) such that,

$$J\dot{\omega}_t = \tau_h - B\omega_t - \tau_c \tag{1}$$

where τ_h is a nonlinear function of the turbine operating point. Turbine τ_h takes the form,

$$\tau_h = \frac{1}{2} C_q(\lambda) \rho A_t R_t u^2 \tag{2}$$

in which ρ is the water density, A_t is the turbine's swept area, R_t its radius, u is the inflow velocity, and C_q is the torque coefficient – a function of the tip-speed-ratio (λ). A turbine operating point (θ) is defined as a stationary velocity and rotation rate pair,

$$\theta = (\bar{u}, \bar{\omega}_t) \tag{3}$$

such that,

$$\lambda = \frac{\bar{\omega}_t R_t}{\bar{u}} \tag{4}$$

allowing a value of τ_h to be determined from a characteristic performance curve (Fig. 2). This curve is approximated by fitting a cubic polynomial,

$$C_q(\lambda) = a\lambda^3 + b\lambda^2 + c\lambda + d \tag{5}$$

where a, b, c, and d are empirical coefficients. Deviation of measured velocity from the mean is a turbulent perturbation velocity,

$$\hat{u} = u - \bar{u}. \tag{6}$$

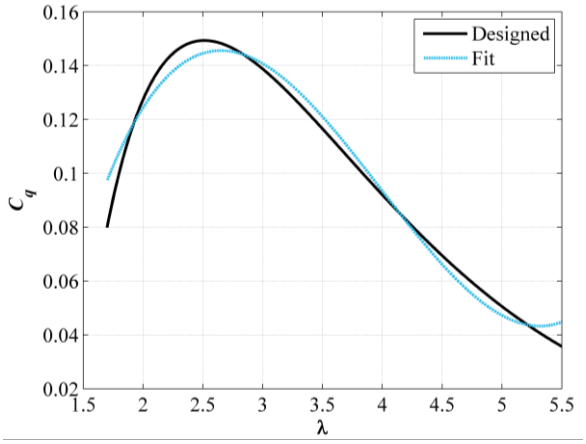

FIGURE 2: Designed and fit torque coefficient characteristic curves for DOE RM2.

The nonlinearity in (2) as a result of (5) can be treated by linearizing (2) around a value of θ, resulting in an expression for fluctuations of τ_h as a result of fluctuations in u and ω_t,

$$\hat{\tau}_h = K_\omega \hat{\omega}_t + K_u \hat{u} \tag{7}$$

where K_ω and K_u are derivatives of τ_h, the result of a first-order Taylor Series expansion about θ (Ginter & Pieper, 2011). These derivatives,

$$K_\omega = \left.\frac{\partial \tau_h}{\partial \omega}\right|_\theta \tag{8}$$

$$K_u = \left.\frac{\partial \tau_h}{\partial u}\right|_\theta \tag{9}$$

take constant values for each value of θ such that,

$$K_\omega = \frac{1}{2}\rho A_t \left(R^2 c\bar{u} + 2R^3 b\bar{\omega}_t + \frac{3R^4 a{\bar{\omega}_t}^2}{\bar{u}} \right) \quad (10)$$

$$K_u = \frac{1}{2}\rho A_t \left(2Rd\bar{u} + R^2 c\bar{\omega}_t - \frac{R^4 a{\bar{\omega}_t}^3}{\bar{u}^2} \right) \quad (11)$$

from substitution of (4) in (5) and then in (2). The linearized version of (1) is then constructed as,

$$\dot{\hat{\omega}}_t = \frac{(K_\omega - B)\hat{\omega}_t}{J} + \frac{K_u \hat{u}}{J} - \frac{\hat{\tau}_c}{J} \quad (12)$$

describing deviation in the rotational acceleration relative to an operating point as a result of deviations in rotation rate and control torque, and turbulence. The linearized dynamic system of (12) can be represented as a state space model that varies with θ, a first-order linear parameter varying (LPV) system where,

$$\dot{\hat{\omega}}_t = A(\theta)\hat{\omega}_t + B_1(\theta)\hat{u} + B_2\hat{\tau}_c$$
$$\hat{\omega}_t = C\hat{\omega}_t + D\hat{\tau}_c \quad (13)$$

with coefficients,

$$A = \frac{K_\omega - B}{J}, B_1 = \frac{K_u}{J}, B_2 = \frac{1}{J},$$
$$C = 1, D = 0 \quad (14)$$

and the single state and output variable, $\hat{\omega}_t$ (Ginter & Pieper, 2011). The open-loop response of the turbine can be evaluated using standard linear time invariant (LTI) system techniques at any static value of θ. The system can thus be treated as a linear combination of transfer functions – one relating fluctuations in rotation rate to turbulence, and a second relating fluctuations in rotation rate to deviation in control torque,

$$\hat{\omega}_t = [G_1(s) \quad G_2(s)] * [\hat{u} \quad \hat{\tau}_c]^T \quad (15)$$

the combination of which yields the total fluctuation in rotation rate (Bianchi et al., 2007). $G_1(s)$ and $G_2(s)$ are obtained from (13) as,

$$G_1(s) = C(sI - A)^{-1}B_1 + D = \frac{K_u/J}{s + \left(\frac{B - K_\omega}{J}\right)} \quad (16)$$

$$G_2(s) = C(sI - A)^{-1}B_2 + D = \frac{1/J}{s + \left(\frac{B - K_\omega}{J}\right)} \quad (17)$$

both of which have an identical single pole. The simplified system is analogous to a low-pass filter, where the location of the pole determines the slope of the turbine's response roll-off. The transfer functions are evaluated in the frequency domain to yield the turbine response in terms of magnitude and phase shift. The magnitude of the transfer function indicates the gain by which the state variable (deviation in rotation rate) increases relative to the inputs (turbulence or control torque fluctuations). A physical intuition for the phase response can be gained by imagining the inputs and outputs as purely sinusoidal; the phase shift is the amount (in degrees) by which the output response wave is shifted from the input when viewed in the time domain.

2. Determining System Response Sensitivity

The turbine's dynamic response is sensitive to the turbine's physical parameters. These parameters may be tuned in the design phase of a system to meet certain control requirements. To exemplify the effect, the turbine is scaled by factors (k) between 0.5 and 2 to create a family of geometrically-scaled models. Using the simplifying assumption that turbine blades can be approximated as solid cylinders of uniform density, blade height, chord length (cylinder diameter), and turbine radius scale with k resulting in blade (and turbine) mass scaling by k^3. Using the definition of the moment of inertia of a solid cylinder rotating about an axis parallel to its own, blade inertia is approximated as

$$J_{blade} = \frac{mc^2}{8} + \frac{mR_t^2}{2} \quad (18)$$

where c is the blade chord length and m is the blade mass, J scales by a factor of k^5.

3. Quantifying Turbulence of a Tidal Channel Flow

Analysis of the flow in a tidal channel is conducted to determine if the turbulent

frequencies the RM2 is sensitive to would be present in the flow during operation. Velocity time-series data collected at 32 Hz with a Nortek Vector Acoustic Doppler Velocimeter (ADV) moored 10 m above the seabed in 56 m deep water near Admiralty Inlet in Washington's Puget Sound is utilized for this analysis (Thomson et al., 2013). The time-series contains the periodic changes in velocity associated with the site's mixed semidiurnal tidal cycle over the span of a day (Fig. 3). Velocity cycles through each of the turbine's operating states: below cut-in speed (< 0.7 m/s), above cut-in but below rated speed (≥ 0.7, < 2 m/s), and above rated (≥ 2 m/s). A relatively stationary 10 minute portion of this data is selected near the turbine's rated flow speed during flood tide with a mean horizontal velocity of 1.93 m/s. A linear trend is subtracted from the time-series to remove non-turbulent variation. The horizontal velocity is de-spiked to remove spurious points according to a 3D phase-space algorithm (Mori et al., 2007). The time-series is split into windows of 128 s with 50% overlap and processed with a Hamming filter prior to performing an FFT and merging the spectra to obtain a single turbulence spectrum (Thomson et al., 2013). The magnitude of the resulting spectrum represents the turbulent kinetic energy (TKE) present in the flow over the frequency band of interest.

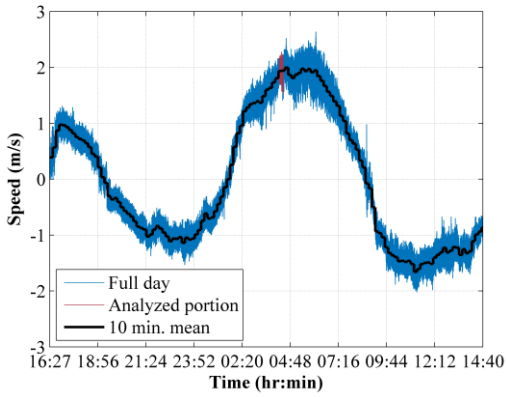

FIGURE 3: Horizontal velocity time series: Admiralty Inlet site.

KEY FINDINGS

1. TURBINE OPEN-LOOP RESPONSE

Evaluating the transfer functions (16) and (17) over a range of frequencies of turbulence and fluctuations of control torque respectively yields the system open-loop response in terms of magnitude and phase shift. A value of the operating point is chosen near the rated speed of the turbine and at optimal λ of 3.15 so that θ = [1.93 m/s, 1.88 rad/s].

The resulting Bode plot is shown in Fig. 4. The frequency at which turbulence induces a 1:1 gain on $\hat{\omega}_t$ (zero-crossing frequency) is 0.67 Hz. The magnitude of the response to $\hat{\tau}_c$ ($G_2(s)$) appears low due to scale – torque in the range of kNm is developed by the turbine. The plots indicate the turbine should uniformly respond to turbulence and control actions up to frequencies of 0.1 Hz before the response diminishes. The roll-off in response occurs at the same frequencies for both G_1 and G_2 due to their single common pole.

Sensitivity of the response to the operating point is evaluated by performing the same analysis at different values of λ. Values are selected to the left and right of the maximum power point (MPP) at λ = 3.15. Bode plots for these responses are shown in Fig. 5, where only the response to turbulence is presented. The turbine responds similarly while operating to the right of the MPP at λ = 4.15. To the left of the MPP at λ = 2.15, we observe the phase shift is -180°, at which point any positive turbulent fluctuation would induce a negative rotation rate perturbation (antiphase response), and approaching a gain of 0 dB, indicating the system may not be open-loop stable based on Nyquist stability criteria (Nise, 2011). This is consistent with observations of operating turbines experiencing hydrodynamic stall at values of λ lower than the value at the MPP, while maintaining stability above this value.

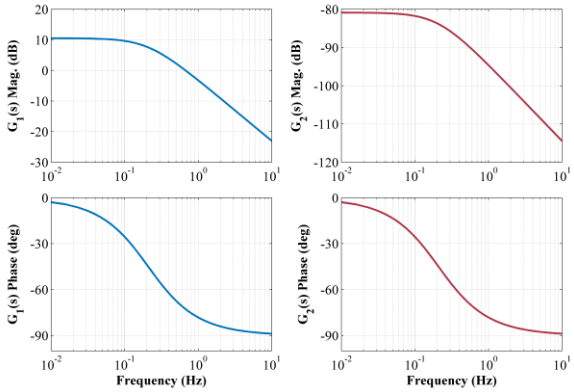

FIGURE 4: Frequency response at near-rated conditions: response to turbulence (left) and deviation in control torque (right).

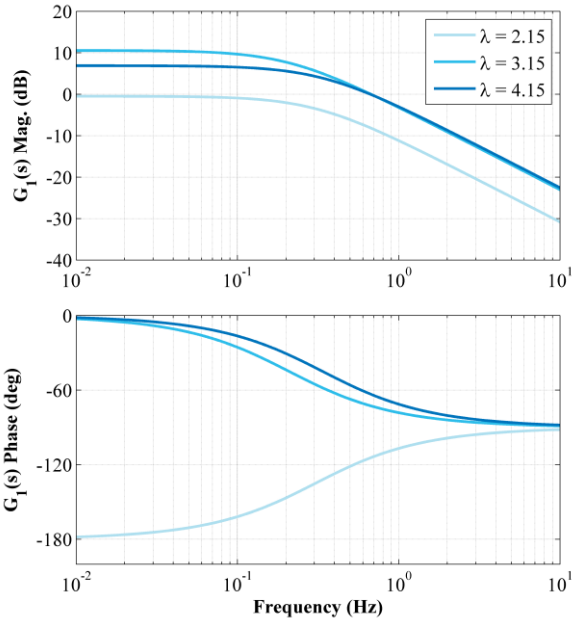

FIGURE 5: Frequency response to turbulence: variation with operating point.

2. SENSITIVITY TO TURBINE PARAMETERS

Turbine scaling factors are applied and the dynamic response to turbulence according to transfer function G_1 is evaluated (Fig. 6). Turbines of smaller dimensions and inertia have a higher magnitude sensitivity to turbulence as well as significant response over a larger frequency band. Turbines larger than the base dimensions are correspondingly less sensitive to turbulence over all bands and exhibit significant response over a smaller band of frequencies. The scaling technique applied assumes the turbine characteristic curve of (5) remains unchanged with scale.

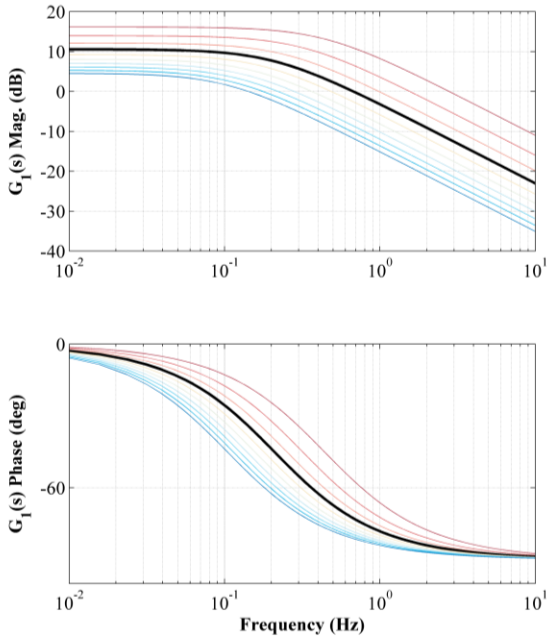

FIGURE 6: Frequency response to turbulence at near-rated conditions: variation with turbine scale – red to blue, smallest to largest, black full scale.

3. TIDAL TURBULENCE

The spectrum of TKE at the Admiralty Inlet site (Fig. 7) contains three distinct regimes: below 0.1 Hz, the lowest frequency, anisotropic turbulent structures contain the most energy, between 0.1 and 2 Hz there is a classic isotropic eddy cascade, and above 2 Hz the turbulence spectra is masked by Doppler noise inherent to instrument operation (Thomson et al., 2012). Several aspects of the impact of turbulence on control can be observed by viewing the turbine's response to turbulence and the turbulence spectrum together (Fig. 8). The turbine is most capable of reacting to turbulence at frequencies with the most intense TKE.

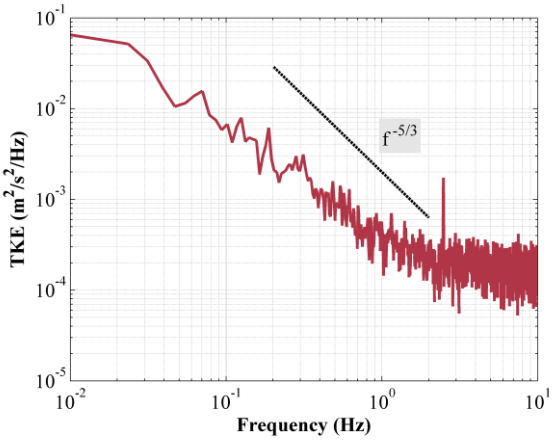

FIGURE 7: Horizontal TKE: 10 minutes with mean of 1.93 m/s, Admiralty Inlet site.

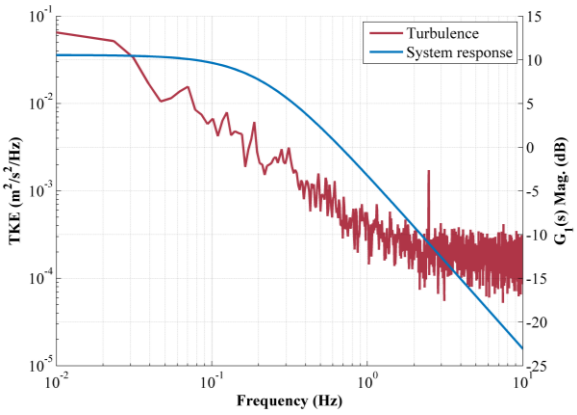

FIGURE 8: Turbulence spectrum and DOE RM2 response to turbulence.

At the frequency of unity gain (0.67 Hz), the magnitude of TKE is reduced to 0.7% of its value at 0.01 Hz. In the inertial subrange, the turbine response decreases at nearly the same rate as the TKE with the chosen magnitude units. Correlating turbulence frequencies to length scales (L) assuming Taylor's frozen field assumption so that,

$$L = \frac{\bar{u}}{f} \tag{19}$$

where f is the frequency of turbulence, indicates eddies between 3 m and 250 m in length are capable of inducing a greater than unity gain in rotation rate fluctuations (Taylor, 1937). These are length scales on the order of the physical dimensions of the turbine and greater. The turbine is significantly less sensitive to turbulence at smaller length scales.

CONCLUSIONS

A method for linearizing the dynamics of a fixed-pitch hydrokinetic turbine is presented. As this type of system is relatively simple, the resulting model consists of just a single state and output, a control input, and a disturbance. This method describes fluctuations about an operating point only, therefore the process must be repeated at a number of operating points to determine how the turbine would respond under different conditions.

Adjusting the tip speed ratio of operation is the simplest way to change the operating point. It is shown that operation at the turbine's maximum power point and at higher rotation rates is stable. Operation at slower speeds begins to become unstable at speeds lower than that corresponding to the peak of the C_q/λ curve. This instability manifests a hydrodynamic stall, which decreases the energy production capability of the turbine and should be minimized by a robust controller.

A use of understanding the turbine's response to turbulence for control is determining the frequency of perturbations that are worth responding to, in terms of control effort to power production enhancement. It is clear that, due to the variation of the mean flow over times scales of hours, a control strategy should include adjustment to switch between operational regimes, possibly achieved through the methods of gain scheduling. Additionally, it is shown that a control strategy adjusting to achieve an operational set-point on the order of seconds may be desirable, as the water speed is highly variable on this time scale. This suggests measuring the disturbance (turbulence) could be beneficial for control. Finally, adjustment to track turbulence beyond roughly 1 Hz appears to be of little benefit, as the turbine's ability to respond at this rate is low and the amount of energy available at these frequencies is also low.

The turbine parameters primarily driving dynamic response are radius and rotational moment of inertia. These parameters may be tweaked in the design stage of a turbine to yield a desired open-loop response. An additional feature determining the response is the turbine's characteristic curve. For a fixed-pitch turbine, this curve is ideally constant. Adjusting blade pitch results in altering the curve in the C_q/λ plane, and thus altering the turbine's dynamics. Similar methods employed to visualize the effects of scaling the turbine could be used to evaluate the effects of blade pitch on a turbine's response to turbulence.

ACKNOWLEDGEMENTS

Velocity time series data was generously provided by J. Thomson and B. Polagye of NNMRC. Many thanks to them and their team for the work. Thanks to B. Polagye and D. Murray for review and comments. This research was supported by the Department of Energy (DOE) Office of Energy Efficiency and Renewable Energy (EERE) Postdoctoral Research Awards under the EERE Water Power Program administered by the Oak Ridge Institute for Science and Education (ORISE) for the DOE. ORISE is managed under DOE contract number DE-AC05-06OR23100. All opinions expressed in this paper are the author's and do not necessarily reflect the policies and views of DOE, ORAU, or ORISE

REFERENCES

Barone, M., Griffith, T., & Berg, J. (2011). Reference Model 2: "Rev 0" Rotor Design SAND2011-9306. Albuquerque, NM.

Bianchi, F. D., De Battista, H., & Mantz, R. (2007). Wind Turbine Control Systems: Principles, Modeling and Gain Scheduling Design. Springer-Verlag London Limited. (p. 83-91).

Cavagnaro, R., Fabien, B., & Polagye, B. (2014). Control of a Helical Cross-Flow Current Turbine. In Proceedings of the 2nd Marine Energy Technology Symposium, METS 2014, April 15-18. Seattle, WA.

Ginter, V. J., & Pieper, J. K. (2011). Robust Gain Scheduled Control of a Hydrokinetic Turbine. IEEE Transactions on Control Systems Technology, 19(4), 805–817.

Mori, N., Suzuki, T., & Kakuno, S. (2007). Noise of Acoustic Doppler Velocimeter Data in Bubbly Flows. Journal of Engineering Mechanics, 133(1), 122–126.

Neely, J. C., Ruehl, K. M., Jepsen, R. A., Roberts, J. D., Glover, S. F., White, F. E., & Horry, M. L. (2013). Electromechanical Emulation of Hydrokinetic Generators for Renewable Energy Research. In OCEANS'13 MTS/IEEE. San Diego.

Nise, Norman S. (2011). Control Systems Engineering, Sixth Edition. John Wiley & Sons, Inc., Hoboken, NJ. (p. 576-580).

Taylor, G. I. (1937). The statistical theory of isotropic turbulence. J. Aero- naut. Sci., vol. 4, (p. 311–315).

Thomson, J., Kilcher, L., Richmond, M., Talbert, J., DeKlerk, A., Polagye, B., Cienfuegos, R. (2013). Tidal turbulence spectra from a compliant mooring. In Proceedings of the 1st Marine Energy Technology Symposium, METS 2013. Washington, D.C.

Thomson, J., Polagye, B., Durgesh, V., & Richmond, M. C. (2012). Measurements of Turbulence at Two Tidal Energy Sites in Puget Sound, WA. IEEE Journal of Oceanic Engineering, 37(3), 363–374.

Whitby, B., & Ugalde-loo, C. E. (2014). Performance of Pitch and Stall Regulated Tidal Stream Turbines. IEEE Transactions on Sustainable Energy, 5(1), 64–72.